Preparation and Characterization of DNA Containing a Site-Specific Nonadjacent Cyclobutane Thymine Dimer of the Type Implicated in UV-Induced −1 Frameshift Mutagenesis†

Jody M. Lingbeck and John-Stephen Taylor*

Department of Chemistry, Washington University, St. Louis, Missouri 63130

Received May 6, 1999; Revised Manuscript Received August 5, 1999

ABSTRACT: One mechanism for the origin of UV-induced −1 deletion mutations involves the bypass of a nonadjacent cis-syn cyclobutane pyrimidine dimer containing a single intervening nucleotide. To begin to investigate this mechanism, we required a method for obtaining a single, site-specific, nonadjacent dimer. One approach to the preparation of a nonadjacent dimer is to irradiate a DNA duplex containing a centrally located TNT sequence in which the two T's are paired to an AA sequence in an otherwise fully complementary strand. Triplet-sensitized irradiation of the duplex formed between the 13-mer d(GAGTATCTATGAG) and the 12-mer d(CTCATAATACTC) on ice gave a major product that could be reverted to the parent 13-mer by 254 nm irradiation. Proton NMR experiments established the major product to be the nonadjacent cis-syn cyclobutane dimer formed between the two T's of the TCT sequence. Melting temperature studies show that the nonadjacent dimer is more destabilizing to DNA duplex structure than a normal cis-syn dimer and is as stable as the parental bulged DNA duplex. The nonadjacent dimer-containing 13-mer was ligated into a 51-mer and used as a template for primer-extension studies by DNA polymerases. The nonadjacent dimer could not be bypassed by Sequenase Version 2.0 and terminated synthesis primarily prior to and opposite the 3′-T of the dimer. In contrast, approximately 30% of the dimer was bypassed by an exonuclease-deficient (exo$^-$) Klenow fragment, and termination occurred primarily opposite the 3′- and 5′-T's of the dimer. Bypass of the nonadjacent dimer by exo$^-$ Klenow fragment led primarily to a single-nucleotide deletion mutation as well as small amounts of a full-length product and a four-nucleotide deletion that could be explained by a primer misalignment mechanism.

UV light is known to induce substitution, addition, and deletion mutations. Single-nucleotide deletion mutations account for 30−35% of the observed UV-induced mutations in the *lacI* gene of *Escherichia coli* which had been irradiated with 254 nm light (*1*). A_n·T_n sequences in the *lacI* gene are hotspots for −1 frameshift mutations (*1*, *2*) as well as for the formation of cis-syn dimers (*3*). Based on these results, a strand slippage model involving cis-syn dimers in T-tracts was proposed to account for the observed −1 frameshift mutations (*2*). In support of this model, single and double deletion mutations along with a misalignment-mediated substitution mutation were observed when a T_6-tract containing a thymine dimer in the second position was bypassed by the exo$^-$ T7 DNA polymerase Sequenase Version 2.0 (*4*).

Another intriguing proposal for the origin of UV-induced single-nucleotide deletion mutations involves the replicative bypass of a nonadjacent cyclobutane dimer (*5*) which results from dimerization between two stacked pyrimidines that flank a bulge loop (Figure 1A). In support of such a mechanistic possibility, irradiation of single-strand, alternating poly[d(G·T)] or poly[d(C·T)] sequences with 254 nm light was shown to produce cis-syn dimers as the major isomer, but in only 1% yield (*5*). The yield of nonadjacent dimers (NADs)[1] could be increased to 40% with the use of wavelengths >280 nm and a triplet sensitizer such as acetone (*6*). Nonadjacent dimers have also been shown to form in poly[d(A·T)] in which the duplex form has been destabilized by manganese chloride or 60% ethanol (*7*). Nonadjacent CC dimers, which contain an extrahelical thymine, have been prepared in low yield by annealing poly[d(T·C)] to poly-[d(G·G·A)] to create a hybrid duplex in which alternating thymines were excluded and irradiating with 254 nm light (*8*). To investigate the role of nonadjacent dimers in UV-induced deletion mutations, a method for preparing a single, site-specific nonadjacent dimer in good yield is required. Herein, we report the preparation and characterization of a nonadjacent thymine dimer with an intervening C, and show that the major product of trans lesion synthesis by an exonuclease-deficient Klenow fragment of DNA polymerase I of *E. coli* is a single nucleotide deletion.

† This work was supported by NIH Grant CA-40463, and in part by NIH Biomedical Research Support Shared Instrument Grants RR-02004, RR-05018, and RR-07155 in support of the Washington University High-Resolution NMR facility.

* To whom correspondence should be addressed. Phone: (314) 935-6721. FAX: (314) 935-4481. Email: taylor@wuchem.wustl.edu.

[1] Abbreviations: [*c*,*s*], cis-syn stereochemistry of the cyclobutane ring of a pyrimidine cyclobutane dimer; DTT, dithiothreitol; dNTP, deoxynucleotide triphosphate; exo$^-$, 3′-5′ exonuclease deficient; NAD, nonadjacent dimer; NOESY, nuclear Overhauser effect spectroscopy; N^X[*y*,*z*]N, nonadjacent cyclobutane dimer with the extrahelical sequence X and with [*y*,*z*] stereochemistry; TOCSY, total correlation spectroscopy; TSP, trimethylsilylpropionate.

10.1021/bi991035i CCC: $18.00
Published on Web 09/23/1999

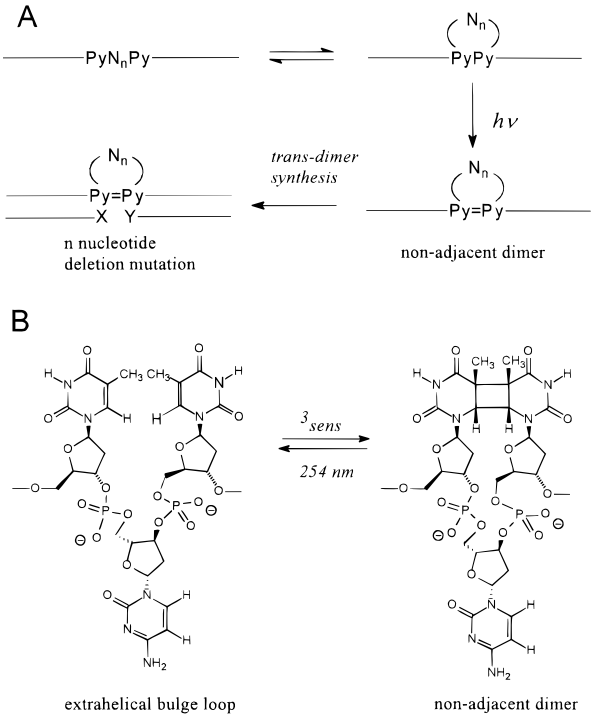

FIGURE 1: (A) General scheme for the formation of *n* nucleotide deletion mutations by formation and bypass of nonadjacent dipyrimidine photoproducts. (B) Specific nonadjacent cis-syn cyclobutane dimer prepared in this study by triplet-sensitized irradiation of TCT in a 13-mer complexed to a complementary 12-mer lacking the complementary G.

MATERIALS AND METHODS

Enzymes, Reagents, and Equipment. All oligonucleotides were purchased from Integrated DNA Technologies. DNA concentrations were determined by the absorbance at 260 nm using estimated molar extinction coefficients (*9*). T4 polynucleotide kinase, T4 DNA ligase, and *Mbo*II were purchased from New England Biolabs. Exonuclease-deficient Klenow fragment of DNA polymerase I [D355A, E357A (*10*)] was obtained from United States Biochemical (USB) (10 units/μL, 0.25 mg/mL). 3′→ 5′ exonuclease-deficient T7 DNA polymerase [Sequenase 2.0, Δ28 K118−R145 (*11*)] was purchased from USB (13 units/μL, 11 μM). *E. coli* thioredoxin was obtained from Promega. [γ-^{32}P]ATP (10 μCi/μM) was purchased from Amersham. Reverse phase HPLC was performed on a Dynamax C-18 column (4.6 × 250 mm for analytical work and 10 mm × 250 mm for semipreparative work). NMR spectra were obtained on a Varian UNITY 600 MHz spectrometer and processed on a SPARC 10 computer using VNMR software. Melting temperature curves were acquired on a Cary 1E UV−visible spectrometer fitted with a multicell block and Peltier cooling pumps and interfaced to a Pentium computer using Cary Win UV software (WIN95 version) to collect and process the data. Melting point bath oil, density 0.96 g/mL and viscosity 200 centistokes at 25 °C, was purchased from Sigma. Nonlinear least-squares curve fitting was done by the Kaleidagraph program. Radioactive bands in gels were detected with a Molecular Dynamics storage phosphor screen (35 × 43 cm), analyzed by a Molecular Dynamics phosphorimager, model 425S, and processed by ImageQuant software.

Preparation and Isolation of the Nonadjacent Dimer. d(GAGTATCTATGAG) (~1 μmol) was annealed to an equimolar amount of d(CTCATAATACTC). The duplex was dissolved in 3.3 mL of photolysis buffer (100 mM NaCl, 10 mM phosphate, 30 mM acetophenone, 15% CH_3CN in H_2O) to give a final DNA concentration of 300 μM. The sample was divided into two NMR tubes (which served as a Pyrex filter) and degassed by bubbling N_2 through the solution for 5 min. Photolysis was carried out for 4 h at 0 °C at wavelengths >290 nm using a Hanovia medium-pressure mercury arc lamp. After photolysis, the samples were combined, concentrated, and separated by semipreparative, C-18, reverse-phase HPLC using a 50 min 8−32% gradient of methanol in K_2HPO_4/KH_2PO_4 (pH 6.7) at a flow rate of 2.3 mL/min. The fractions were concentrated and desalted on the same column by washing with water for 20 min and eluting with 50% aqueous CH_3CN. The isolated yield of the nonadjacent dimer containing oligomer was 0.018 μmol.

^{1}H NMR Experiments. NMR spectra for the nonadjacent dimer-containing single-strand NAD-13-mer were acquired in 0.3 mL of a 50 μM solution in D_2O at 25 °C. The spectra were referenced to the HOD signal, which was assigned to 4.79 ppm. An ^{1}H TOCSY spectrum (*12*) was acquired in the phase-sensitive mode by employing the Hypercomplex method (*13*). Data were collected in a 2 × 270 × 1984 data matrix by using a 50 ms MLEV-17 mixing sequence preceded by a 2 ms trim pulse with 32 scans per t_1 value. Two-dimensional Fourier transformation was carried out following Gaussian-weighted line broadening in both t_1 and t_2 dimensions to give a 2000 × 2000 data set which was phase-corrected in both dimensions. The ^{1}H NOESY spectrum (*14, 15*) of the nonadjacent dimer-containing duplex (NAD-13-mer·AA-12-mer) was acquired on a 0.3 mL sample of 0.12 mM DNA, 250 mM NaCl, 10 mM phosphate, 0.1 mM NaN_3, and 0.2 mM EDTA in D_2O at 5 °C. The spectrum was acquired in the phase sensitive mode by employing the Hypercomplex method (*13*) and referenced to TSP at 0.0 ppm. The data were collected into a 2 × 270 × 1984 matrix using a 100 ms mixing time and 64 scans per t_1 value, and then zero-filled to give a 2000 × 2000 data set that was phase-corrected in both dimensions. Gaussian-weighted line broadening was employed prior to Fourier transformation in both t_1 and t_2 dimensions.

Melting Temperature Experiments. UV melting temperature experiments were carried out in 1 M NaCl, 10 mM sodium cacodylate (pH 7.0), and 0.1 mM EDTA at total single-strand concentrations of approximately 15, 7.5, and 3.75 μM in an 80 μL 1 cm path length quartz cuvette and topped off with 100 μL of melting point bath oil. The sample compartment was flushed with N_2 to prevent water condensation on the cells at low temperatures, and the absorbance was monitored at 260 nm between 2 and 80 °C. The duplex was thermally anneal prior to data acquisition. Denaturation and renaturation curves for the duplex were collected with a heating and cooling rate of 0.5 °C/min. Thermodynamic parameters were derived by nonlinear least-squares fitting of the UV melting temperature curves (*16*).

Preparation of the Templates. Oligonucleotides purchased from IDT were purified by gel electrophoresis. 1.5 nmol of the nonadjacent dimer oligomer and 1.5 nmol of the 21-mer were phosphorylated separately with 10 units of T4 polynucleotide kinase in 20 μL of kinase buffer (70 mM Tris·HCl, 10 mM $MgCl_2$, 5 mM DTT, pH 7.6) containing 25 nmol of ATP (Figure 2). The reactions were incubated at

37 °C for 1 h and quenched by heating the tubes at 100 °C for 5 min to deactivate the enzyme. The phosphorylated 13-mer and 21-mer were added to 1.5 nmol each of the 17-mer and the 36-mer ligation scaffold. The sequences were annealed and lyophilized and resuspended in 30 μL of ligase buffer (50 mM Tris·HCl, 10 mM $MgCl_2$, 10 mM DTT, 1 mM ATP, and 50 μg/mL BSA, pH 7.8) containing 800 units of T4 DNA ligase. The reaction was incubated overnight at 4 °C and electrophoresed on a 15% denaturing polyacrylamide gel. The desired 51-mer template was eluted from the gel and ethanol-precipitated.

Primer Extension Reactions. The 14-mer primer (7 pmol) was 5′-end-labeled with 10 units of T4 polynucleotide kinase in 14 μL of kinase buffer containing 6.7 pmol (10 μCi/mL) of [γ-^{32}P]ATP. The reaction was incubated for 1 h at 37 °C and quenched by denaturing the enzyme at 100 °C for 5 min. Primer extension reactions with exo$^-$ KF (30 units for dimer templates and 16 units for nondimer templates) were conducted on 1 pmol of primer/template in 15 μL of 50 mM Tris·HCl (pH 7.5), 10 mM $MgCl_2$, 10 mM DTT, and 100 μM of each dNTP. Primer extension reactions with Sequenase Version 2.0 (1.5 μM final concentration plus an additional 20 equiv of reduced *E. coli* thioredoxin) were carried out on 1 pmol of primer/template in 15 μL of 40 mM Tris·HCl (pH 7.5), 20 mM $MgCl_2$, 50 mM NaCl, 5 mM DTT, and 100 μM in each dNTP. The reactions were incubated at 37 °C for 1 h followed heating at 100 °C for 5 min and another 5 min on ice. *Mbo*II cleavage of the primer-extension products was carried out on 4 μL of the reaction mixture by addition of 1 unit of enzyme and enough NaCl to make the final concentration 50 mM. Cleavage reactions were incubated at 37 °C for 30 min and quenched with 5 μL of 95% formamide. The reaction products were run on a 15% polyacrylamide gel and imaged. Dideoxy sequencing was carried out with a 1:3 ddNTP:dNTP ratio on 0.5 pmol of the labeled 14-mer primer that was annealed to 1.5 pmol of the 51-mer template that did not contain a dimer. The percent bypass was calculated as the volume integral of the full-length bypass products divided by the volume integral for all the extension products determined by phosphoimager analysis of the gels. The distribution of full-length and deletion bypass products was determined by volume integration of the 21−25-mer bands resulting from cleavage with *Mbo*II and then subtracting the volume of the background bands. The volumes of the background band volumes were calculated on the basis of the percentages of these same bands that were observed in the uncleaved sample.

RESULTS AND DISCUSSION

Experimental Design. One can envision two general approaches to prepare DNA containing site-specific nonadjacent pyrimidine photodimers with reasonable efficiency. The most general approach would be to synthesize a nonadjacent photodimer building block that could be incorporated into DNA site-specifically and sequence-independently by standard automated DNA synthesis. This approach is rather difficult and has not yet succeeded in our laboratory. Another approach with more limited sequence generality is based on the methods used to prepare nonadjacent dimers in DNA polymers (*5*−*7*, *17*), and that is to irradiate a synthetic single-strand oligonucleotide containing a sequence that can only yield a unique nonadjacent pyrimidine dimer.

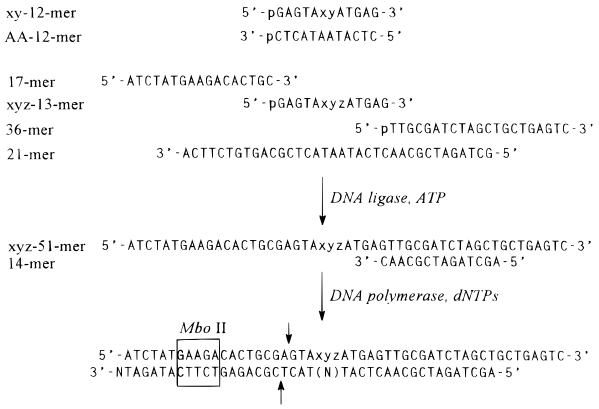

FIGURE 2: Oligonucleotides and substrates used in this study, where xy = TT or an adjacent TT dimer (T[*c*,*s*]T), and xyz = TCT or a nonadjacent dimer (T^C[*c*,*s*]T). A 50-mer template was also constructed from the TT and T[*c*,*s*]T-12-mers.

The highest yield of nonadjacent dimers in single-strand DNA has been obtained by triplet-sensitized irradiation with acetone [40% yield for poly [d(GT)] (*6*)]. In this case, however, a substantial amount of trans-syn isomers (14%) was produced in addition to the cis-syn dimer. It has also been shown that nonadjacent dimers can be formed between two C's in poly[d(TC)] by duplex formation with a template strand that is complementary to the two C's but only one of the T's, poly[d(GGA)] (*8*). The efficiency of nonadjacent dimer formation in a bulge loop-containing duplex is expected to depend on the extent to which the duplex adopts a structure in which the two nonadjacent pyrimidines are stacked and the intervening nucleotide is extrahelical. In this regard, it has been found that single pyrimidine bulges tend to be extrahelical (*18*−*21*), and single purine bulges intrahelical (*22*, *23*). It has also been found that pyrimidine bulges which have been shown to exist in both intrahelical and extrahelical forms at room temperature become more extrahelical as the temperature is lowered (*18*, *21*).

With these basic design criteria in mind, we chose to examine the triplet-sensitized photochemistry of the 13-mer d(GAGTATPyTATGAG) in the presence and absence of the complementary 12-mer d(CTCATAATACTC). At low temperatures, these two strands are expected to form a duplex containing a single extrahelical pyrimidine nucleotide bulge. The advantage of a TT sequence is that a cyclobutane dimer at this site can be selectively produced in the presence of C-containing dipyrimidine sites by triplet-sensitized irradiation with acetophenone (*24*). We therefore chose C as the intervening pyrimidine nucleotide because a T could lead to three possible sensitized products: the desired nonadjacent dimer, as well as two adjacent dimers. The C-bulge-inducing template (AA-12-mer), though having a number of dipyrimidine sites, had no TT sites and was not expected to lead to any photoproducts under triplet-sensitized irradiation. The sequence flanking the TCT site in the TCT-13-mer (Figure 2) was based on the TT-12-mer sequence that had been previously designed to have only a single dipyrimidine site (the TT site) to enable the preparation of site-specific (6−4) and Dewar photoproducts by direct irradiation (*25*). In addition, thermodynamic data were obtained for these photoproducts and for the cis-syn dimer which could be compared to that of the nonadjacent dimer.

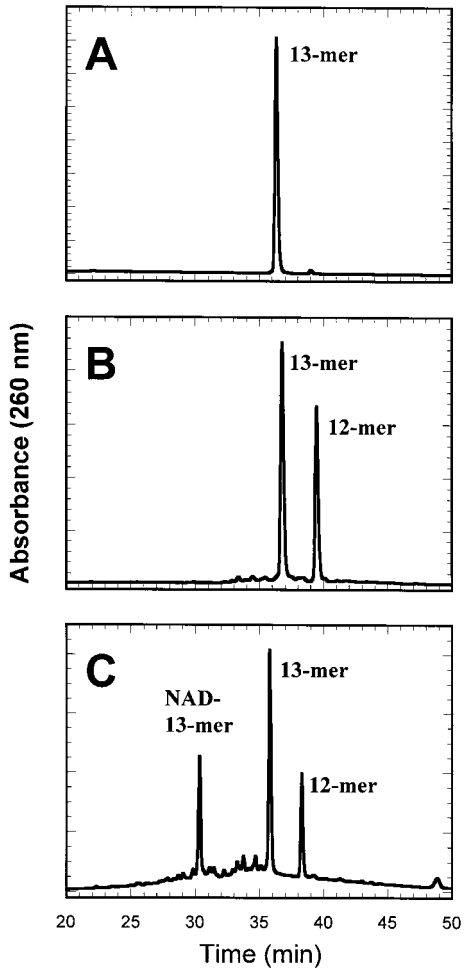

FIGURE 3: HPLC traces of (A) the parent TCT-13-mer, (B) the parent TCT-13-mer/AA-12-mer duplex, and (C) the reaction mixture after 4 h irradiation of the TCT-13-mer/AA-12-mer duplex with Pyrex-filtered medium-pressure mercury arc light at 0 °C in the presence of acetophenone.

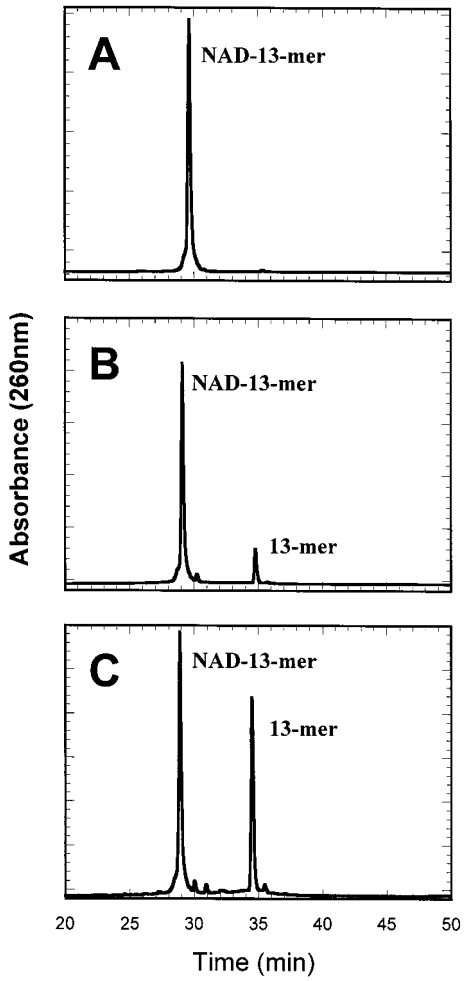

FIGURE 4: HPLC traces of a solution of the nonadjacent dimer-containing 13-mer before (A) and after (B) 1 min and (C) 3 min irradiation with 254 nm light at 0 °C.

Triplet-Sensitized Formation of the Nonadjacent Dimer. Pyrex-filtered irradiation of the duplex at 0 °C with >290 nm light in the presence of the triplet sensitizer acetophenone gave rise to only one major photoproduct in about 14% yield by HPLC peak integration which eluted faster than either the AA-12-mer or the TCT-13-mer (Figure 3). A large number of smaller peaks were also observed which are presumably photoproducts of the CTC sequences in the complementary strand that arise by direct absorption of the UV light. This would also explain why the size of the AA-12-mer peak decreased when compared to the TCT-13-mer peak. To establish the nature of the major photoproduct formed, we made use of the fact that cyclobutane dimers can be reversed by 254 nm light, whereas other classes of photoproducts are not (*26*). Irradiation of the purified photoproduct with 254 nm light for 1 and 3 min caused photoreversion back to the 13-mer and not to the 12-mer (Figure 4), demonstrating that it was a photoproduct of the 13-mer. ^{1}H NMR (Figure 5) was used to further characterize the photoproduct in comparison to the NMR of the parental TCT-13-mer. The aromatic region shows the loss of two aromatic TH6 protons upon irradiation, consistent with saturation of the C6 carbons that occurs upon formation of the cyclobutane ring fusion. The upfield shift of the two methyl signals is also consistent with a change in hybridization of C5 from sp^2 to sp^3 that would accompany formation of a cyclobutane ring and is typical for cyclobutane dimers of TpT in dinucleotides and single-strand DNA (*27*, *28*). Evidence that the C5−C6 double bond of the cytosine is not involved in photoproduct formation is further established by a 2D TOCSY experiment (Figure 6A). A cross-peak appears with chemical shifts typical of native cytosine, indicating that the C5−C6 double bond remains intact and is not involved in cyclobutane dimer formation.

Stereochemistry of the Nonadjacent Dimer. To determine the stereochemistry of the cyclobutane ring, NOESY spectra were acquired on the nonadjacent dimer-containing 13-mer to look for NOE's between the cyclobutane methyl and H6 protons. If the two T's were base-paired to the two A's on the complementary strand during photodimerization, the cis-syn stereochemistry would be expected, and NOE's between the two methyls should be observed. Also, an NOE between at least one methyl and both H6 protons should also be observed depending on pucker and flexibility of the ring (*29*, *30*). On the other hand, if one of the two T's was rotated 180° relative to the other one during photodimerization, a trans-syn dimer would result, and only NOE's between the methyl group and the H6 of the same pyrimidine ring system should be observed. NOE's between the two methyls or between one of the methyls and both H6 protons should not be observed.

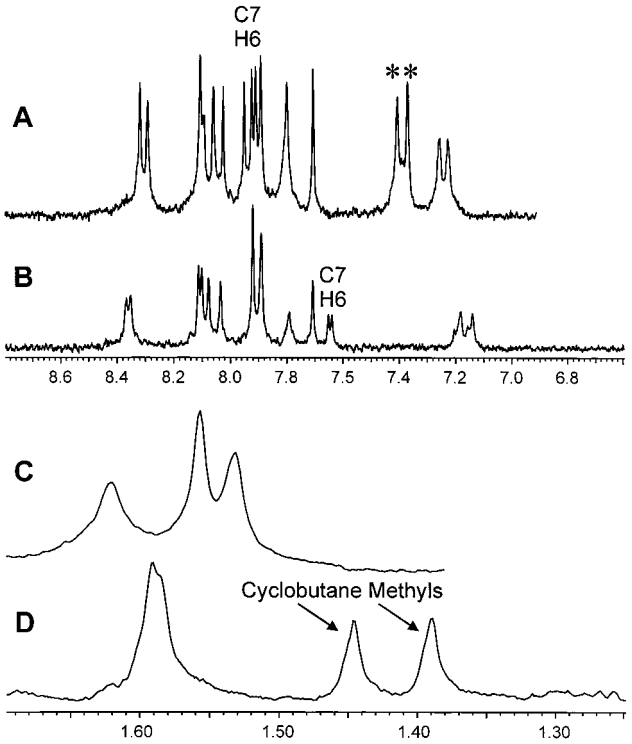

FIGURE 5: Sections of the one-dimensional ^{1}H NMR spectrum of (A) the parent TCT-13-mer and (B) the nonadjacent dimer-containing TCT-13-mer showing the loss of two aromatic TH6 protons and the upfield shift of two TCH_3 methyl signals.

A NOESY spectrum of the single-strand nonadjacent dimer-containing 13-mer was not good enough to firmly establish the stereochemistry of the cyclobutane ring of the dimer, in part because of the small chemical shift difference between the two methyls, and because of poor signal-to-noise. Because duplex formation causes the shifts of the methyl signals of adjacent cyclobutane thymine dimers to spread apart due to differential ring current effects from the flanking bases (*29*, *31*−*33*), the NOESY spectrum was also acquired on the duplex formed between the NAD-13-mer and the AA-12-mer. As observed for adjacent cis-syn thymine dimer-containing duplexes (Table 1), one of the methyl signals in the duplex moved upfield to 0.62 ppm, and showed a cross-peak to a methyl signal at 1.46 ppm (Figure 6B). These two methyl signals had cross-peaks with signals at 4.00 and 4.35 ppm, typical of the shifts of H6 signals of cyclobutane thymine dimers (Table 1). The pattern of cross-peaks between the methyl and H6 signals of the nonadjacent dimer-containing duplex is also typical of cis-syn thymine dimer-containing duplexes (*29*, *32*), with one methyl signal (1.46 ppm) showing strong cross-peaks to both H6 protons. This type of pattern arises from a preferred cyclobutane ring conformation with a right-handed twist (CB^+) (*29*, *30*).

The cis-syn stereochemistry of the nonadjacent thymine dimer formed when the TCT-13-mer was annealed to the AA-12-mer is consistent with the formation of an extrahelical C bulge loop structure in which the two nonadjacent T's were stacked and base-paired to the two A's. Crystal structures of bulge loop duplexes with an extrahelical nucleotide show that the nucleotides flanking the extrahelical nucleotide stack in a B-like conformation (*34*, *35*). Likewise, irradiation of duplex DNA results almost exclusively in adjacent thymine cyclobutane dimers with the cis-syn stereochemistry, and it is only when single-strand DNA is irradiated that any significant amount of dimer with the trans-syn stereochemistry is produced (*24*).

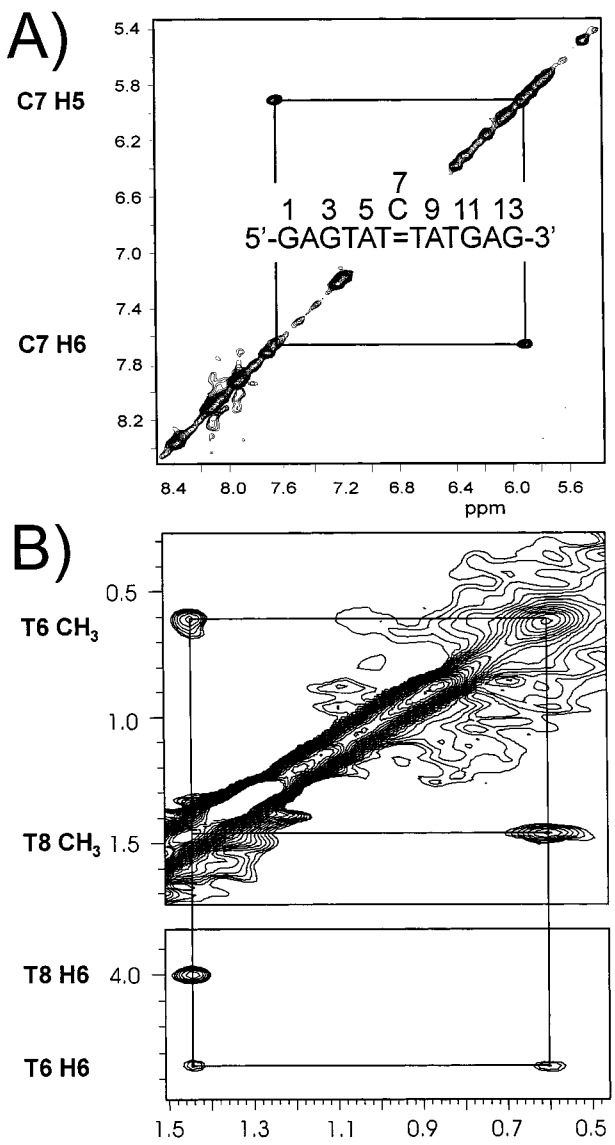

FIGURE 6: Sections of (A) the 50 ms TOCSY spectrum of the nonadjacent dimer-containing TCT-13-mer at 25 °C showing the correlation between the aromatic CH5 and CH6 proton signals expected for a nondimerized cytosine, and (B) a 100 ms NOESY spectrum of the nonadjacent dimer-containing TCT-13-mer annealed to the complementary AA-12-mer at 5 °C showing correlations between the T6 and T8 methyl and H6 proton signals.

Table 1: Chemical Shifts of the Methyl and H6 Protons of Adjacent and Nonadjacent Thymine Dimers in DNA Duplexes

	5′-TCH_3	3′-TCH_3	5′-TH6	3′-TH6
d(CGTAT[*c*,*s*]TATGC)· d(GCATAATACG)[a]	0.51	1.48	4.48	4.12
d(GCGT[*c*,*s*]TGCG)· d(CGCAACGC)[b]	0.71	1.53	4.48	4.10
d(GAGTAT^C[*c*,*s*]TATGAG)· d(CTCATAATACTC)[c]	0.62	1.40	4.35	4.00

[a] Taylor et al. (*29*). [b] Kemmink et al. (*31*). [c] This study. Assignments are made by comparison of chemical shifts to those of duplexes containing adjacent cis-syn cyclobutane thymine dimers.

Table 2: Thermodynamic and Melting Temperature Data for the Formation of the Parent, Adjacent Dimer, and Nonadjacent Dimer Containing Duplexes in 1 M NaCl[a]

duplex	$\Delta G°$ (kcal/mol)	$\Delta\Delta G°$ (kcal/mol)	T_M at 15 μM (°C)	ΔT_M (°C)
TT·AA[b]	−10.6	−	49	−
T[*c,s*]T·AA[b]	−9.1	1.5	43	−6
TCT·AA	−6.9	3.7	33	−16
T^C[*c,s*]T·AA	−6.6	4.0	32	−17

[a] Free energies are calculated for 37 °C. ΔT_m is relative to the parent dodecamer. [b] Jing et al. (*25*).

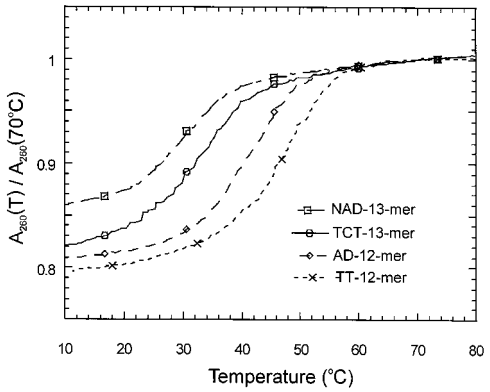

FIGURE 7: Normalized melting temperature curves for duplexes formed between the AA-12-mer and the nonadjacent dimer-containing TCT-13-mer (NAD-13-mer) and its parental strand (TCT-13-mer), in comparison to the curves for the adjacent cis-syn thymine dimer containing TT-12-mer (AD-12-mer) and its parental strand (TT-12-mer), all at approximately 15 μM concentration.

Thermodynamic Properties. The thermodynamic properties of the nonadjacent dimer-containing duplex and its undamaged parental duplex were obtained by analysis of the shape of the UV melting temperature curves (*16*) and compared to data for the adjacent cis-syn dimer (Table 2) (*25*). The thermodynamic parameters for the bulge loop and nonadjacent dimer-containing duplexes are almost identical and lower in magnitude than those for the TT-12-mer and adjacent dimer-containing duplexes (Figure 7). The drop in stability of the bulge-containing duplex relative to the parent ($\Delta\Delta G$ = 3.7 kcal, ΔT_m = 16 °C) is quite similar to that previously reported for a C bulge flanked by two T's ($\Delta\Delta G$ = 3.9 kcal, ΔT_m = 16 °C) (*36*). Whereas the adjacent dimer only decreases the free energy of duplex formation by 1.5 kcal/mol and the T_m by 6 °C, the nonadjacent dimer is much more disruptive to duplex formation ($\Delta\Delta G$ = 4.0 kcal, ΔT_m = −17 °C) and is more similar in effect to the bulge loop.

A number of factors have been suggested to be responsible for the lower stability of bulge loop containing duplexes relative to the duplexes without the bulged nucleotide. It has been found that bulge loops take up more counterions than the non-bulge loop containing duplexes and also cause a larger volume contraction. These effects have been attributed to the higher charge density and/or increase in solvation due to the presence of an extrahelical nucleotide (*37*). Some of these effects may also play a role in destabilizing a nonadjacent dimer relative to an adjacent dimer, though they may not be as great because the extrahelical loop is already present in the nonadjacent dimer-containing single strand. Preorganizing the extrahelical loop by dimer formation would be expected to reduce the entropic penalty for forming the loop in the duplex form as well as reducing both favorable and unfavorable terms related to complexation of ions and hydration of the extrahelical bulge. It is also possible that the two T's in the nonadjacent dimer have a different conformation than in the adjacent dimer which may also affect free energy terms relating to pi-stacking and base-pairing.

Mutagenic Potential of the Nonadjacent Dimer. The mutagenic potential of the nonadjacent dimer was investigated by ligating the NAD-13-mer into a 51-mer template (Figure 2) for primer-extension studies by well-characterized polymerases known to bypass the cis-syn dimer and other dipyrimidine photoproducts. For comparison purposes, the adjacent dimer-containing TT-12-mer was also ligated to form a 50-mer. In previous studies, we have found that the cis-syn dimer, and, to a lesser extent, the trans-syn-II, (6−4), and Dewar photoproducts, can be bypassed by 3′-5′ exonuclease-deficient (exo$^-$) T7 DNA polymerase and by an exo$^-$ Klenow fragment (*38*). Abolishing the exonuclease activity of these polymerases greatly enhances their ability to bypass photoproducts (*4*, *38*, *39*), as well as other types of DNA damage (*40*), making it possible to study otherwise infrequent events. Because exonuclease-deficient polymerases are known to carry out nontemplated addition of nucleotides to the blunt end of a fully extended product (*41*, *42*), it is not possible to discriminate accurately between full-length and deletion bypass products. To solve this problem, an *Mbo*II site was engineered into the 3′-side of the template to allow the variable 3′-end of the bypass product to be removed (Figure 2). Under these conditions, a full-length bypass product of the nonadjacent dimer will appear as a 25-mer, and of the adjacent dimer as a 24-mer.

The nonadjacent dimer severely inhibited bypass by both Klenow fragment and Sequenase Version 2.0 in comparison to the adjacent dimer (17% and 6% vs 80% and 79% in the uncleaved lanes). In contrast to what we previously found for the adjacent cis-syn dimer, which was more easily bypassed by Sequenase Version 2.0, the nonadjacent dimer was bypassed more easily by the exo$^-$ Klenow fragment (Figure 8). When the bypass products of the nonadjacent dimer were cleaved by *Mbo*II and corrected for background bands, it was found that the majority of the products was the single-nucleotide deletion (11%), with smaller amounts of the full-length product (4%) and an interesting four-nucleotide deletion (7%). The single-nucleotide deletion is what would be expected if the polymerase uses the two T's of the nonadjacent dimer as the template, and the extrahelical C is ignored, as proposed by Nguyen and Minton for the origin of −1 frameshift mutations (*5*). The four-nucleotide deletion was originally unanticipated, but can be seen to arise as a consequence of a slippage or misalignment event (Figure 9). The nonadjacent dimer is part of the triplet repeat sequence TATTAT if one ignores the extrahelical C. Synthesis up to the nucleotide prior to the 3′-T of the dimer would create a primer terminating in AT opposite the upstream triplet which could misalign and base-pair with the AT in the downstream triplet and continue synthesis. Alternatively, it is known that Klenow fragment preferentially introduces an A opposite the 3′-T, and this is also expected to hold true for the nonadjacent dimer. In this case, the primer terminating in ATA opposite the upstream triplet could likewise misalign with the downstream triplet and continue synthesis.

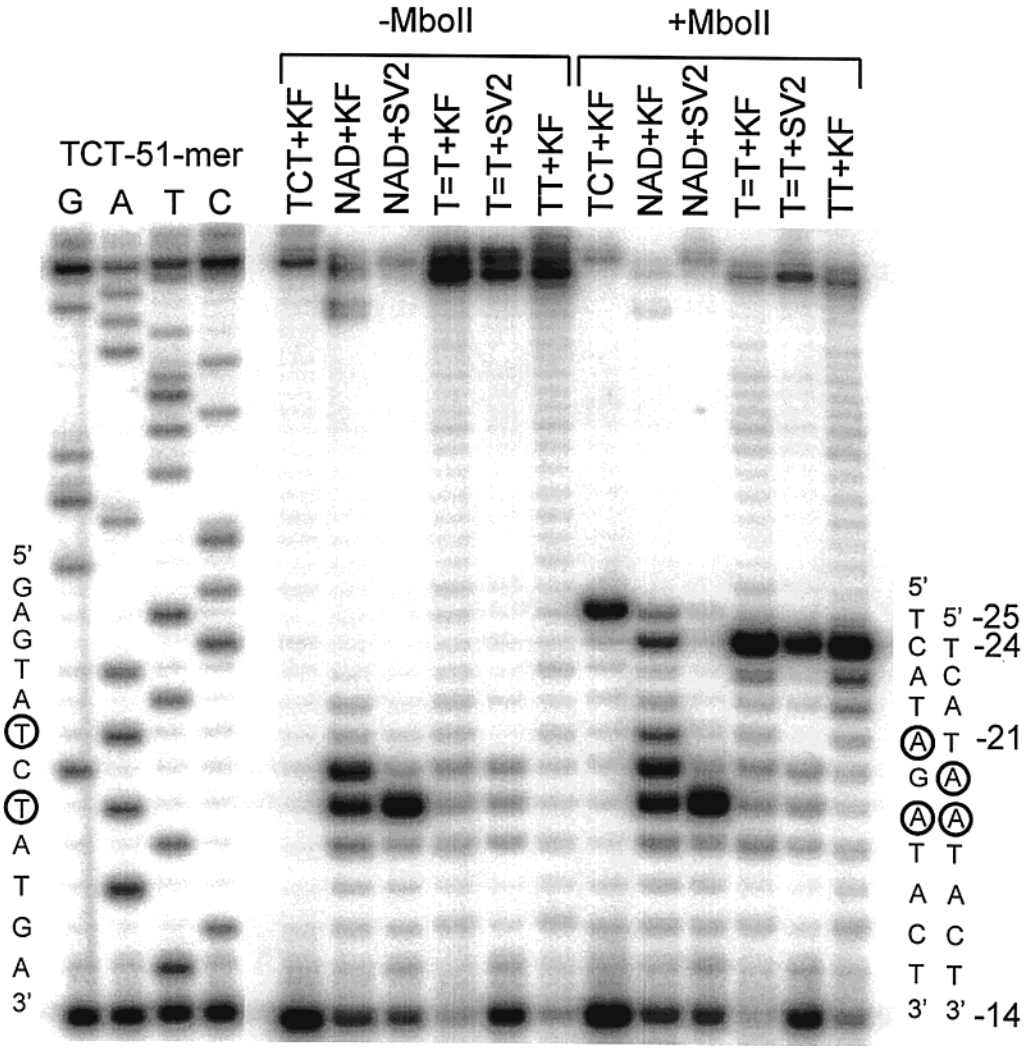

FIGURE 8: Image of a denaturing electrophoresis gel of the radiolabeled products of primer extension experiments opposite the 51-mer templates containing the nonadjacent dimer (NAD) and its parental strand (TCT), and opposite 50-mer templates containing the adjacent TT dimer (T=T) and its parental strand (TT). The primer extension reactions were performed with exo$^-$ Klenow fragment (KF) and Sequenase Version 2.0 (SV2) with and without subsequent cleavage by *Mbo*II. The dideoxynucleotide sequencing reactions were performed on the parental TCT 51-mer template, whose sequence is shown on the left in which the two T's forming the nonadjacent dimer are circled. The sequence of the primer extension product opposite the 50-mer template containing two adjacent T's is shown on the far right, and to its left, the sequence of the extension product opposite the TCT-51-mer, in which the two A's that would be incorporated opposite the two T's are circled. The 25-mer band corresponds to the product of error-free primer-extension opposite the TCT-51-mer followed by *Mbo*II cleavage whereas the 24-mer band corresponds to *Mbo*II cleavage of a −1 frameshift error. The 24-mer band also corresponds to the product of error-free primer-extension opposite the TT-50-mer.

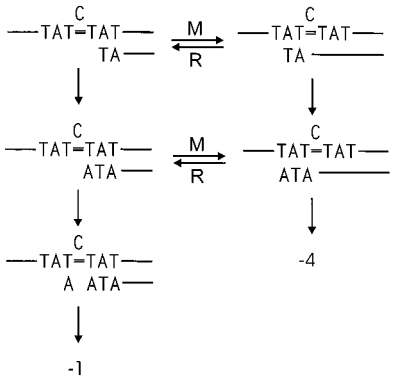

FIGURE 9: Possible mechanisms for the origin of the −1 and −4 mutations produced by the nonadjacent dimer. M indicates a misalignment step and R a realignment step.

The −4 mutation was not observed for bypass by Sequenase 2.0 or for bypass of the adjacent dimer by either polymerase in the same triplet repeat context. It would appear that when the rate of in-register elongation past the damage site is severely decreased, then the alternate pathway leading to the −4 mutation becomes viable for the Klenow fragment, but not for Sequenase 2.0. The mechanistic origin of the full-length product that was produced in 4% yield is not understood at the moment, and may be due to contamination by a small amount of adjacent TC or CT dimer. In such a case, Sequenase 2.0 should have been able to readily bypass it, but in the *Mbo*II cleavage assay, only about 0.5% of the full-length product was observed to be produced along with 1% of the −1 product. No significant amounts of −2, −3, or −4 products were detected with Sequenase 2.0.

The switch in the relative ability of the Klenow fragment and Sequenase to bypass photodamage was also seen with the TA* photoproduct (*43*). In that case, exo$^-$ Klenow fragment was able to bypass the TA* product, though elongation of primers terminating opposite the A and T of

the photoproduct was very slow. Likewise, exo$^-$ Klenow was able to bypass the nonadjacent dimer, though elongation of primers terminating opposite either T of the dimer was very slow. In contrast, Sequenase Version 2.0 was not able to bypass the TA* photoproduct, and synthesis terminated primarily opposite the A and the nucleotide to the 3′-side of the A of the photoproduct. Likewise, Sequenase 2.0 was not able to bypass the nonadjacent dimer, and synthesis terminated primarily opposite the 3′-T of the nonadjacent dimer. It is possible that the two photoproducts place similar conformational or steric demands on the two polymerases which are different from those imposed by an adjacent cis-syn dimer.

Conclusions. We have developed a method for preparing a nonadjacent dimer and demonstrated that it can indeed lead to −1 frameshift mutations as originally proposed by Nguyen and Minton (*5*) with exo$^-$ Klenow fragment. Whether or not a nonadjacent dimer will also cause this mutation in *E. coli* under SOS or non-SOS conditions, or in the cells of higher organisms, can now be tested because a site-specific substrate is now available. The nonadjacent dimer also can function as a conformationally locked extrahelical loop which could be used to test mechanisms in which otherwise conformationally mobile bulge loops have been proposed as intermediates in a variety of −1 frameshift mutagenesis mechanisms. It may also serve a method for preparing conformationally locked loops of larger size that can be used to study recognition of such loops in DNA and RNA by a wide variety of proteins.

ACKNOWLEDGMENT

We thank Yingie Ren for a sample of the adjacent dimer-containing 12-mer, and Jeffrey Kao for help with the NMR experiments.

REFERENCES

1. Miller, J. H. (1985) *J. Mol. Biol. 182*, 45−68.
2. Schaaper, R. M., Dunn, R. L., and Glickman, B. W. (1987) *J. Mol. Biol. 198*, 187−202.
3. Brash, D. E., and Haseltine, W. A. (1982) *Nature 298*, 189−192.
4. Wang, C.-I., and Taylor, J.-S. (1992) *Biochemistry 31*, 3671−3681.
5. Nguyen, H. T., and Minton, K. W. (1988) *J. Mol. Biol. 200*, 681−693.
6. Nguyen, H. T., and Minton, K. W. (1989) *J. Mol. Biol. 210*, 869−874.
7. Love, J. D., and Minton, K. W. (1992) *J. Biol. Chem. 267*, 24953−24959.
8. Evans, D. H., and Morgan, A. R. (1982) *J. Mol. Biol. 160*, 117−122.
9. Fasman, G. D. (1975) *Handbook of Biochemistry and Molecular Biology. Nucleic Acids−Volume I*, CRC Press, Cleveland.
10. Derbyshire, V., Freemont, P. S., Sanderson, M. R., Beese, L., Friedman, J. M., Joyce, C. M., and Steitz, T. A. (1988) *Science 240*, 199−201.
11. Tabor, S., and Richardson, C. C. (1989) *J. Biol. Chem. 264*, 6447−6458.
12. Bax, A., and Davis, D. G. (1985) *J. Magn. Reson. 65*, 355−360.
13. States, D. J., Haberkorn, R. A., and Ruben, D. J. (1982) *J. Magn. Reson. 48*, 286−292.
14. Kumar, A., Ernst, R. R., and Wuthrich, K. (1980) *Biochem. Biophys. Res. Commun. 95*, 1−6.
15. Macura, S., Huang, Y., Suter, D., and Ernst, R. R. (1981) *J. Magn. Reson. 43*, 259−281.
16. Petersheim, M., and Turner, D. H. (1983) *Biochemistry 22*, 256−263.
17. Kim, S.-T., and Sancar, A. (1995) *Photochem. Photobiol. 61*, 171−174.
18. Kalnik, M. W., Norman, D. G., Li, B. F., Swann, P. F., and Patel, D. J. (1990) *J. Biol. Chem. 265*, 636−647.
19. Morden, K. M., Gunn, B. M., and Maskos, K. (1990) *Biochemistry 29*, 8835−8845.
20. Morden, K. M., and Maskos, K. (1993) *Biopolymers 33*, 27−36.
21. Kalnik, M. W., Norman, D. G., Zagorski, M. G., Swann, P. F., and Patel, D. J. (1989) *Biochemistry 28*, 294−303.
22. Woodson, S. A., and Crothers, D. M. (1988) *Biochemistry 27*, 3130−3141.
23. Kalnik, M. W., Norman, D. G., Swann, P. F., and Patel, D. J. (1989) *J. Biol. Chem. 264*, 3702−3712.
24. Lamola, A. A., and Yamane, T. (1967) *Proc. Natl. Acad. Sci. U.S.A. 58*, 443−446.
25. Jing, Y., Kao, J. F.-L., and Taylor, J.-S. (1998) *Nucleic Acids Res. 26*, 3845−3853.
26. Wang, S. Y. (1976) *Photochemistry and Photobiology of Nucleic Acids: Volume I, Chemistry*, Vol. 1, Academic Press, Inc., New York.
27. Liu, F.-T., and Yang, N. C. (1978) *Biochemistry 17*, 4865−4876.
28. Taylor, J.-S., Brockie, I. R., and O'Day, C. L. (1987) *J. Am. Chem. Soc. 109*, 6735−6742.
29. Taylor, J.-S., Garrett, D. S., Brockie, I. R., Svoboda, D. L., and Telser, J. (1990) *Biochemistry 29*, 8858−8866.
30. Kim, J.-K., and Alderfer, J. L. (1992) *J. Biomol. Struct. Dyn. 9*, 705−718.
31. Kemmink, J., Boelens, R., Koning, T. M. G., Kaptein, R., van der Marel, G. A., and van Boom, J. H. (1987) *Eur. J. Biochem. 162*, 37−43.
32. Kim, J.-K., Patel, D., and Choi, B.-S. (1995) *Photochem. Photobiol. 62*, 44−50.
33. McAteer, K., Jing, J., Kao, J., Taylor, J. S., and Kennedy, M. A. (1998) *J. Mol. Biol. 282*, 1013−1032.
34. Joshua-Tor, L., Rabinovich, D., Hope, H., Frolow, F., Appella, E., and Sussman, J. L. (1988) *Nature 334*, 82−84.
35. Miller, M., Harrison, R. W., Wlodawer, A., Appella, E., and Sussman, J. L. (1988) *Nature 334*, 85−86.
36. LeBlanc, D. A., and Morden, K. M. (1991) *Biochemistry 30*, 4042−4047.
37. Zieba, K., Chu, T. M., Kupke, D. W., and Marky, L. A. (1991) *Biochemistry 30*, 8018−8026.
38. Smith, C. A., Baeten, J., and Taylor, J. S. (1998) *J. Biol. Chem. 273*, 21933−21940.
39. Sagher, D., Turkington, E., Acharya, S., and Strauss, B. (1994) *J. Mol. Biol. 240*, 226−242.
40. Eckert, K. A., and Opresko, P. L. (1999) *Mutat. Res. 424*, 221−236.
41. Clark, J. M., Joyce, C. M., and Beardsley, G. P. (1987) *J. Mol. Biol. 198*, 123−127.
42. Clark, J. M. (1988) *Nucleic Acids Res. 16*, 9677−9686.
43. Zhao, X., Kao, J. L. F., and Taylor, J.-S. (1995) *Biochemistry 34*, 1386−1392.

BI991035I